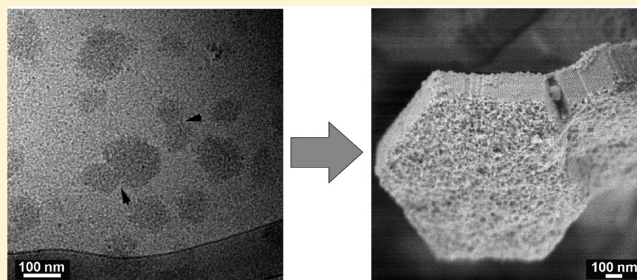


## Transient Colloidal Stability Controls the Particle Formation of SBA-15

Juanfang Ruan,<sup>†,||</sup> Tomas Kjellman,<sup>\*,†</sup> Yasuhiro Sakamoto,<sup>‡,§</sup> and Viveka Alfredsson<sup>†</sup><sup>†</sup>Physical Chemistry, Lund University, P.O. Box 124, 221 00 Lund, Sweden<sup>‡</sup>Department of Materials and Environmental Chemistry, Stockholm University, 106 91 Stockholm, Sweden<sup>§</sup>Nanoscience and Nanotechnology Research Center, Osaka Prefecture University, Sakai, Osaka 599-8570, Japan

## S Supporting Information

**ABSTRACT:** A hypothesis about (transient) colloidal stability as a controlling mechanism for particle formation in SBA-15 is presented. The hypothesis is based on results from both *in situ* and *ex situ* investigations, including cryogenic transmission electron microscopy (cryo-TEM), UV-vis spectroscopy, and dynamic light scattering (DLS). Cryo-TEM images show that particles grow via the formation of silica–Pluronic–water “flocs”, which coalesce in a seemingly arbitrary manner. Despite this, the final material consists of well-defined particles with a small size distribution. We argue that the interface between the flocs and surrounding media is covered by Pluronic molecules, which provide steric stabilization. As the flocs grow, the coverage of polymers at the interface is increased until a stable size is reached, and that regulates the particle size. By targeting the characteristics of the Pluronic molecules, during the on-going synthesis, the hypothesis is tested. The results are consistent with the concept of (transient) colloidal stability.



## ■ INTRODUCTION

Mesoporous materials have interesting properties for a wide range of applications, ranging from drug-delivery to catalysis.<sup>1–3</sup> To fully make use of these materials, there is a need for rational design to meet specific demands needed for particular applications. An important parameter to control is obviously the mesoscopic structure but other important characteristics that have a large impact on the function of a material are particle size and particle morphology. Less effort has so far been invested in the understanding of the latter aspects. In order to be able to design the mesoporous materials, and not only rely on empirical synthetic knowledge, the formation events need to be chartered and the driving forces understood. With such knowledge at hand, there is a possibility to “master” the formation on a molecular as well as on a nanoscopic level and direct the synthesis to meet specific demands of the material.

The formation process of the mesoporous silica SBA-15 has attracted considerable interest in recent years,<sup>4–11</sup> but the different stages of formation and the driving forces controlling the growth and structure formation are still only partly understood. The material growth process has been investigated with various *in situ* techniques,<sup>5,11,12</sup> in particular small-angle X-ray scattering<sup>4,7,13</sup> and *ex-situ* techniques,<sup>6,14</sup> but even so, some disagreement remains in regard to the initial development of the material. This will be addressed in some detail below. With this objective at hand, we set out to perform the present study where we investigate and discuss how the colloidal stability influences the particle growth.

One complication when comparing the results from various studies focused on the evolution from a micellar solution of the structure directing amphiphilic solution, to the final 2D hexagonal ordered composite material, resides in the fact that different synthesis conditions have been used. The structure directing block copolymer, silica source, acid, concentrations of reagent species, as well as temperature can be varied. Our group typically uses the Pluronic P104 (EO<sub>27</sub>PO<sub>61</sub>EO<sub>27</sub>), as this polymer, in the temperature interval of around 40–70 °C, gives rise to a well-defined *p6mm* structure as well as to well-defined particles with a small size distribution.<sup>15</sup> Even though it is likely that the formation follows very similar paths despite small differences in synthesis conditions, it is not uncomplicated to directly compare results from different investigations.

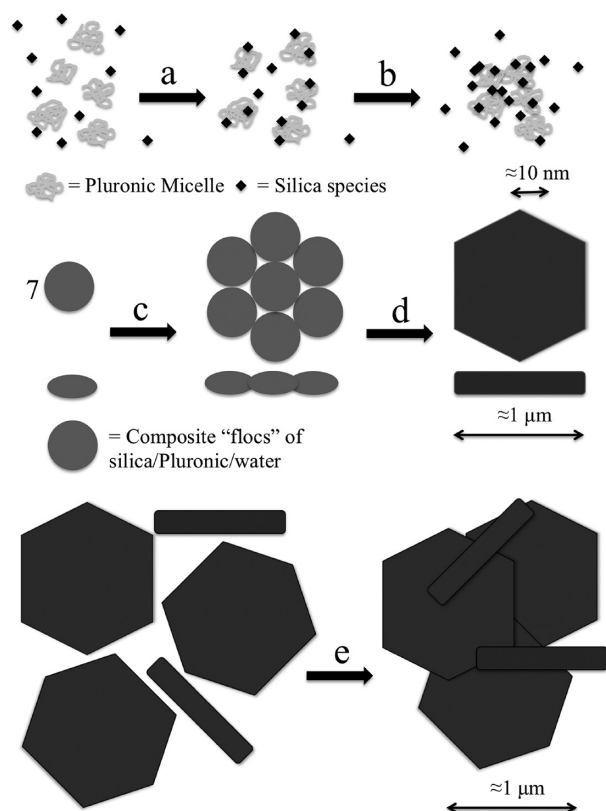
A point of divergence lies in the understanding of how the initial formation takes place. Several reports support a formation relying on an initial growth of spherical micelles to threadlike micelles as silica species associate to the ethyleneoxide chains. These threadlike micelles subsequently aggregate to the ordered structure.<sup>4,6,16</sup> Others, including our group, claim that the initial formation follows a somewhat different path,<sup>11,17,18</sup> and in a recent study,<sup>7</sup> we reported a detailed timeline for these formation events providing opportunities to fine-tune synthesis conditions at certain well-defined times during the synthesis. In Scheme 1 we illustrate

Received: April 5, 2012

Revised: July 3, 2012

Published: July 3, 2012

**Scheme 1. Five Different Steps Suggested To Occur during the Formation of Hexagonal Platelike Particles<sup>a</sup>**



<sup>a</sup>Step a: Association of silica species to the corona of the Pluronic micelles. Step b: Floc-formation and further polymerization of silica species. The flocs are expected to consist of micellar aggregates in a water–silica matrix. Step c: Oriented aggregation of seven flocs to form a secondary particle (“top” and “side” view). Step d: Further cross-linking of silica, rearrangement, and fusing toward the final particle structure and morphology. Step e: Unspecific aggregation of secondary particles to larger aggregates. The increased shading going from the composite flocs of silica/Pluronics/water (c) to the final material (e) is a schematic representation of the increasing density of silica in the developing particles.

our current understanding of the formation events. The association between silica and Pluronic micelles is well-established.<sup>19</sup> This association leads to step a, in Scheme 1. With time, the silica decorated micelles form flocs (step b), and the mesoscopic order is then developed within the flocs as a consequence of micellar growth and reorganization. All our studies, using mainly P104, though also P123 has been used,<sup>10,11</sup> are consistent with this path. In this work we are re-examining these initial stages using mainly cryo-TEM to get direct information on the objects present in the synthesis solution, hence focusing on nucleation and growth. In a number of publications<sup>7,15,20,21</sup> we have described the peculiar, although not unique, particle growth behavior that SBA-15 employs under certain synthesis conditions. Several other types of materials form particles via an oriented growth mechanism,<sup>22</sup> and for some materials this process is highly complex.<sup>23</sup> For SBA-15 this oriented growth step, whereby a heptamer of smaller primary particles (still floclike at this stage) fuses into a large platelike secondary particle (steps c and d, Scheme 1), occurs during the development from unordered flocs to well-ordered SBA-15 particles. This secondary particle is a single

(meso)crystal. A different oriented aggregation behavior is observed at more elevated synthesis temperatures. The particles adhere along the (001) faces forming long rods of stacked particles.<sup>21</sup> Such rods have frequently been observed for SBA-15 materials.<sup>17,24–29</sup>

The secondary particles also undergo unspecific aggregation at later stages of the synthesis (step e, Scheme 1). In this step the identity of the particles is retained but the particles are closely associated with each other. The resulting solution containing SBA-15 particles is hence not a sol of colloiddally stable particles. Instead the aggregated particles exist as a solid precipitate. Silica sols are typically known to have anomalous colloidal stability, and the stability cannot be explained via the DLVO-theory. Although the attractive force is considered to be rather small, as a consequence of a small Hamaker constant, electrostatics do not provide sufficient repulsion to explain the stability. Instead, the stability has been explained to be a consequence of steric effects stemming from oligomeric or polymeric silicate species present at the silica–water interface. Such a layer, which we will henceforth call a brush-layer, will give rise to steric repulsion when the layers overlap.<sup>30</sup> For the flocs and subsequent particles formed in the SBA-15 synthesis, it is clear that the colloidal stability is of a transient nature.

In this study we investigate the early stages of formation of SBA-15 and use cryogenic transmission electron microscopy (cryo-TEM) to visualize the synthesis solution during the early stages of the synthesis (up to 13 min after the addition of the silica source). A number of complementary techniques have also been used, such as UV–vis, DLS, and HRSEM. Based on the results from this investigation as well as those from previous studies, we introduce a hypothesis for a mechanism for the (transient) colloidal stability of flocs and particles in the SBA-15 system. This hypothesis is further assessed in a number of experiments.

## ■ EXPERIMENTAL SECTION

**Synthesis.** SBA-15 was synthesized according to a previously reported protocol<sup>15</sup> which is based on the seminal protocol reported by Zhao et al.<sup>31</sup> but slightly modified. Pluronic P104 (from BASF) is used as structure director, and tetramethyl orthosilicate (TMOS) is used as silica source. TMOS was obtained from Sigma Aldrich. In a typical preparation, Pluronic P104 (0.482 g) was dissolved in 1.6 M HCl (18.75 mL) at room temperature. The solution was then tempered in a water bath to 55 °C followed by TMOS addition (0.715 mL). The resulting mixture was left stirring at this temperature for 24 h and was then placed in an oven at 80 °C for 24 h (static conditions). The final product was filtered and subsequently calcined in an oven at 500 °C for 6 h.

The samples examined at different stages of synthesis time were prepared as above, but the synthesis was terminated at specific sampling times (see the Characterization section).

**Addition of Salt or Polymers.** The standard procedure was followed with a synthesis temperature of 50 or 55 °C. Solutions of NaCl, P104, or F108 in 1.6 M HCl were tempered to the synthesis temperature. A small amount (0.5–1.5 mL) of salt or polymer solution was quickly added in a range of different times to give final concentrations of 0.01, 0.1, 0.25, and 0.5 M NaCl, 5.0 and 10 wt % additional P104, and 1.0 and 2.5 wt % F108, after which the synthesis proceeded as described above. The P104 and F108 concentrations are given with respect to the amount of P104 in a normal synthesis solution (i.e., 0.482 g of P104 is used in the synthesis and 0.048 g of P104 is added for the 10 wt % addition). Dilutions with up to 1.9 mL during a synthesis have previously been shown to be of no consequence for the final material.<sup>20</sup>

**Addition of Silica-Oligomers.** In a modification of the standard procedure, silica oligomers were added to the reaction. A small (0.5–

1.5 mL) addition of a solution containing silica oligomers is made to a normal synthesis 15 min after the initiation by TMOS addition ( $t = 0$  min). The oligomer solution is prepared by addition of TMOS (0.715 mL) to 1.6 M HCl (18.75 g) at 50 °C at  $t = 0$ , -15, -30, and -60 min. A schematic of the experimental procedure is provided in the Supporting Information (SI) (Scheme S1).

**Characterization.** The final product was characterized by small-angle X-ray diffraction (SAXD) using a diffractometer equipped with a position-sensitive detector using nickel-filtered Cu  $K\alpha_1$ . All final products exhibited well-ordered SBA-15 SAXS patterns.

The particle evolution was studied by cryogenic transmission electron microscopy (cryo-TEM) as a function of reaction time (addition of TMOS marks the onset of the synthesis). The specimens for cryo-TEM observations were sampled at different synthesis times. Vitriified specimens were prepared in a controlled environment vitrification system (CEVS) held at the same temperature as the reaction mixture (i.e., 55 °C) and with 100% relative humidity. A small droplet of the solution (9  $\mu$ L) was placed on a holey carbon copper grid, that had previously been glow discharge treated, and excess fluid was removed by gently blotting with a filter paper, immediately followed by vitrification by plunging the grid into liquid ethane (held at -180 °C). The whole process from extracting the droplet from the synthesis solution to quenching the grid in liquid ethane takes on the order of 10 s. Detailed information on cryo-plunging is found in the literature.<sup>32</sup> Specimens were examined in a biotwin Philips CM120 microscope, operated at 120 kV, using an Oxford CT-3500 cryo-holder system. All specimens were observed in the microscope at a temperature below -180 °C. Images were recorded digitally in the low-dose mode by a Gatan 791 MultiScan CCD camera.

HRSEM observations were performed on a JEOL high-resolution scanning electron microscope (JEM-7401F) equipped with an in-lens detector, a gentle beam, and a cold field emission electron source. The microscope was operated at 0.6 kV, and samples were placed on a carbon stub. Freeze-dried specimens for HRSEM observations were first prepared by rapidly freezing the solution at sampling times prior to 30 min of synthesis followed by freeze-drying on a Drywinner 6-85 instrument, at -95 °C under vacuum for 120 h. Normal dried specimens for HRSEM observations were prepared at synthesis times larger than 40 min. The sample was extracted at specific times and immediately diluted 10 times with HCl solution (1.6 M). A drop of the diluted solution was placed onto a TEM grid, and then the grid was blotted with a filter paper. The aim of the dilution here is to make the sample suitable for the imaging. HRSEM was also used on the final calcined material, and in this case the powder was spread on a carbon stub and the images were recorded at 0.4 kV.

SEM micrographs of samples having gone through complete synthesis as well as calcination were recorded with a JEOL JSM-6700 microscope operating at 5 kV. The samples were sputter coated with gold before examination. The SEM micrographs were analyzed regarding the particle size distribution by measuring the distance between parallel sides along the 001 direction of a number of representative particles.

The evolution of the size of the species in the reagent solution was determined *in situ* at 55 °C by DLS with a Malvern instrument (Zetasizer nano ZS). TMOS was added to the Pluronic solution held at 55 °C. The solution was vigorously stirred for about 3 min and then transferred to the measuring cell. The DLS recording started about 2 min later in order to allow for temperature stabilization. The hydrodynamic diameter ( $D$ ) of P104 triblock copolymer (2.5 wt %) in the acidic solution at the synthesis temperature was also determined. Hydrodynamic diameters between 10 and 1000 nm were obtained from the measured diffusion coefficient using the Stokes–Einstein model.

The evolution of the absorbance (i.e., the turbidity) during synthesis was monitored by UV–visible spectroscopy with a Varian instrument (300 Bio spectrophotometer). The preparation of the solution for the measurement was identical to that for the DLS measurement. Moreover, measurements with/without stirring were performed to confirm that the stirring does not affect the final results. Please note

that the solution always went through 3 min of stirring prior to the measurements.

## RESULTS AND DISCUSSION

In this section we first report the results from cryo-TEM, HRSEM, UV–vis, and DLS and relate these results to the current literature. Subsequently we describe a hypothesis to rationalize the observations, and finally we report on the results from experiments aimed at examining the hypothesis.

The results from the investigations are shown in Figure 1 (UV–vis), Figure 2 (DLS), Figure 3 (cryo-TEM), and Figure 4

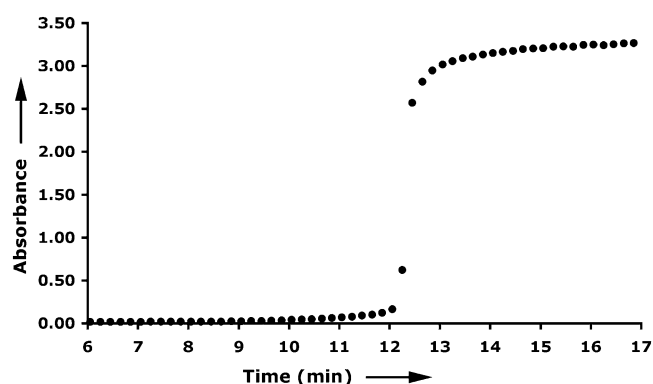


**Figure 1.** Time resolved UV–vis results of the SBA-15 reaction between 6 and 17 min at 55 °C.

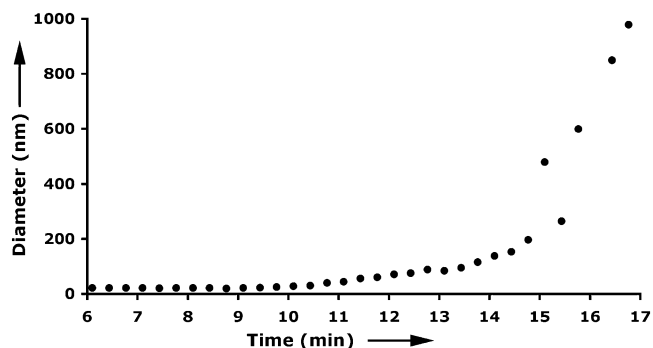


**Figure 2.** Hydrodynamic diameter ( $D$ ) of the species observed during the formation of the SBA-15 at 55 °C.

(HRSEM). The results are from identical syntheses but different batches. Both the UV–vis and the DLS are from *in situ* studies whereas the results from the cryo-TEM and HRSEM investigations are limited to certain sampling times (*ex-situ* investigations). It should be noted that the synthesis is sensitive to temperature deviations.<sup>7,33</sup> A slight temperature difference (estimated to be  $\pm 1^\circ$  between the measurements) may cause minor deviations in times for the formation events for the different batches (techniques). The reproducibility between batches is good, which is clear when comparing the UV–vis results of the 55 °C synthesis previously reported<sup>7</sup> and the one in this report.

The UV–vis spectrum in Figure 1 indicates an increase in absorbance at 9 min indicative of the onset of floc formation.<sup>7</sup> To get more detailed information on the scattering objects in solution, DLS measurements were also performed. Figure 2 shows the hydrodynamic diameter obtained from these measurements (the size distributions by intensity from the



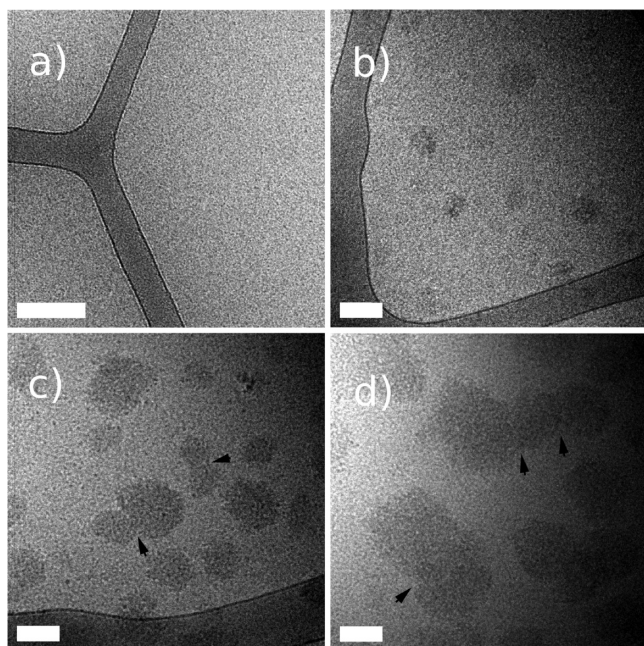


**Figure 3.** Cryo-TEM images of the SBA-15 reaction mixture sampled at a reaction time of (a)  $t = 6$  min, (b)  $t = 9$  min, (c)  $t = 11$  min, and (d)  $t = 13$  min (both reaction and vitrified temperature are  $55^\circ\text{C}$ ). The arrows indicate growth via coalescence of flocs. Scale bar = 100 nm.

DLS measurements are shown in the Supporting Information). These results indicate that the hydrodynamic diameter of the aggregates remains constant to approximately 10 min after the TMOS addition. Following this, an aggregate growth is initially observed, between approximately 11 and 15 min, seen as a gradual increase in the curve, followed, at around 15 min, by a steep increase. The corresponding cryo-TEM results are shown in Figure 3. The samples were extracted from the reagent solution at 6 (a), 9 (b), 11 (c), and 13 (d) min. The micrographs of the 6 min sample (Figure 3a) show no larger aggregates. The vitrified film is consistent with a solution containing globular micelles. It is hard, or even impossible, to identify globular micelles in such a film, but it is likely that threadlike micelles are absent, as these would have been more easily detected. We did not observe any larger objects at this point. Hence, we conclude from the cryo-TEM measurements that the solution at this time (6 min) consists of globular or perhaps slightly elongated micelles. These data support previous findings showing that an initial stage of the formation proceeds via siliceous species adhering to the ethylene oxide (palisade) layers of the spherical Pluronic micelles.<sup>7,11,13,34,35</sup> A few minutes later, at 9 min (Figure 3b), diffuse patches with higher contrast than the surrounding vitrified film are evident from the micrographs. The patches are indicative of globular aggregates with higher electron density than the solution. The size of these aggregates is on the order of 50 nm (approximately 10 times larger than a single micelle). With time, both the contrast and the size of the aggregates have increased, shown in micrographs recorded at 11 (Figure 3c) and 13 (Figure 3d) min, respectively. It should be noted that no internal order could be detected in any of the visualized aggregates at this time. This is in agreement with the previous in situ SAXS study<sup>7</sup> of the same system where the Bragg peaks, indicative of the 2D hexagonal structure, started to emerge only

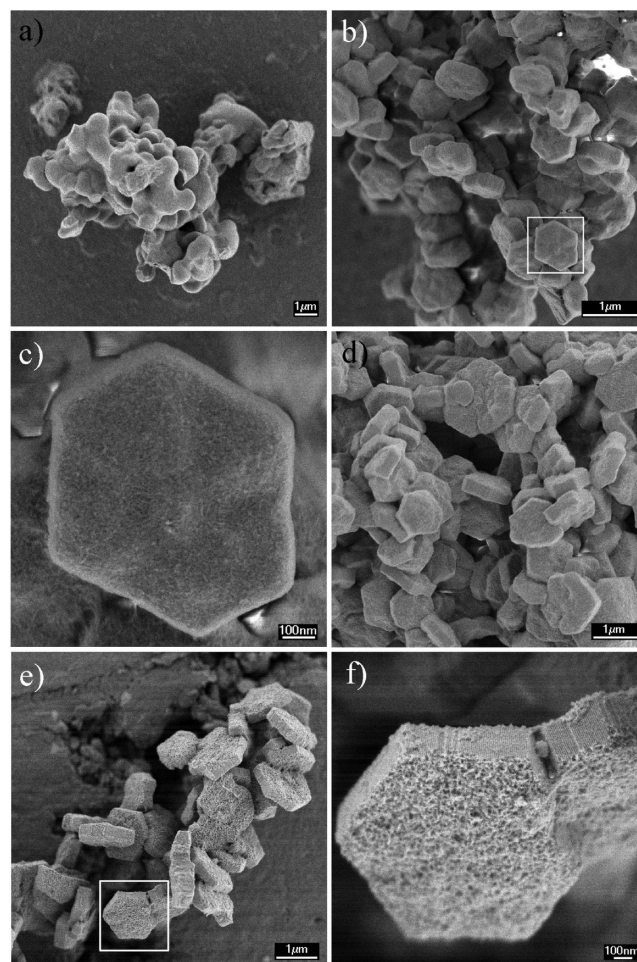


**Figure 4.** HRSEM images of the SBA-15 reaction mixture after a reaction time of  $t$ : (a) freeze-drying sample at  $t = 25$  min, (b) freeze-drying sample at  $t = 29$  min, (c) magnified image of the area marked by the white rectangle in part b, (d) normal drying sample at  $t = 40$  min, (e) calcined sample, and (f) magnified image of the area marked by the white rectangle in part e.

after 14 min. Another interesting observation was made from the micrographs recorded at 11 and 13 min, namely that a number of aggregates were imaged while in the process of coalescing, marked with black arrowheads in Figure 3c and d. (More images are shown in Supporting Information Figures S3–S7.) The time of appearance of the larger aggregates in the cryo-TEM micrographs agrees well with the DLS and UV–vis data.

It was not possible to prepare cryo-TEM samples at later stages of the synthesis, as aggregates had grown too large and a vitrified film could therefore not be obtained. Cryo-TEM as a method is limited to the size of the objects, as these need to be confined within the vitrified film (approximately 500 nm). Instead, HRSEM samples were prepared by freeze-drying the solution. Figure 4 shows the HRSEM images from freeze-dried samples (Figure 4a–c) along with a normal-dried sample (Figure 4d) and a calcined sample (Figure 4e, f). When the solution was extracted 25 min after TMOS addition, the resulting images show globular and closely joined aggregates (Figure 4a). Extraction made a few minutes later, at 29 min (Figure 4b) shows aggregates clearly resembling the calcined particles (cf. Figure 4e). The sample in Figure 4b (magnification in Figure 4c) also has very similar morphology

to that of the sample shown in Figure 4d, which was prepared by normal drying after 40 min of the synthesis. The large difference between Figure 4a and 4b can possibly be explained by a higher degree of silica connectivity in the latter, resulting in more rigid particles. It is also clear that the particle formation is largely complete (i.e., growth completed and morphology matured) after 29 min but possibly earlier. The very fast formation (less than 10 min) of SBA-15 recently reported<sup>14</sup> was not observed in our system. Samples were also extracted (and freeze-dried) at 15 and 20 min and examined in HRSEM. These samples did not show any identifiable particles, likely as a consequence of the particles still being of a very liquid-like nature. Additionally, specimens sampled at 30 and 40 min were also checked in ordinary TEM (see the Supporting Information, Figure S8). These micrographs suggest that the 40 min sample is ordered and the 30 min sample slightly less ordered. In this case the particles had dried before imaging, and this may cause structural changes; however, these results are consistent with the other observations.

From these results we can conclude the following. The initial steps of formation follow a path consistent with formation of flocs, which are unordered in nature, in accordance with previous investigations.<sup>7,11,17</sup> No elongated or wormlike micelles were detected, as was reported in other studies,<sup>4,16</sup> including a previous cryo-TEM investigation.<sup>6</sup> These studies were, however, not performed under identical synthesis conditions as we have used in this work and in our previous studies. Here we note that the formation of particles, including structure and morphology, is completed within the first 29 min of the synthesis (possibly even sooner). Despite the apparent randomness in floc size and the fact that flocs coalesce, a well-defined particle size and shape is obtained; that is, some mechanism must prevail that give rise to growth control.

Before presenting the hypothesis, some previous results should be revisited. As mentioned in the Introduction, SBA-15 can (under certain synthesis conditions) undergo growth via an oriented aggregation step<sup>15</sup> (Scheme 1 step c). Under the conditions used in this report, the growth proceeds via this mechanism (Scheme S2 in the Supporting Information). It has been shown that changes in the solvent conditions can influence this growth step.<sup>20</sup> Addition of simple electrolytes at the point of oriented aggregation generally facilitated this step. However, too much salt resulted in immediate random aggregation and precipitation indicative of the loss of specificity in the aggregation step. It was also found that the aggregation was dependent on the identity of the salt, and hence, the loss of colloidal stability cannot be the result of purely electrostatic arguments (cf. Introduction). It was also shown that the oriented aggregation (step c, Scheme 1) could be avoided by diluting the solution. There is a window of opportunity, limited to a time span of approximately 1–2 min, to influence the oriented aggregation step. After this, the particles are no longer prone to aggregate in an oriented manner.

After completion of synthesis, the material is recovered as a solid precipitate consisting of unspecifically aggregated particles (cf. Figure 4e and step e, Scheme 1). As the final particles are well-defined even though they occur in larger aggregates, this unspecific aggregation must occur once the growth of the individual particles is completed.

From the observations obtained by the in situ as well as ex-situ investigations and, in addition, the results from the previous studies of the nature of the oriented aggregation step, we suggest a hypothesis for the driving forces that control the

particle size. The key observations providing the basis for the hypothesis are summarized here:

(i) The particles grow to a well-defined particle size despite the fact that, according to cryo-TEM, flocs are observed to coalesce and fuse in a random manner. Coalescence in a random manner would typically produce randomly sized particles. For SBA-15, however, the particles have a homogeneous size distribution, inferring that there exists a control mechanism governing the growth. Apparently the growth lasts until the flocs have reached a certain size (approximately 200–300 nm in diameter for the 55 °C synthesis). After this, the oriented aggregation occurs (at certain temperatures, e.g. 55 °C, but not at others).<sup>15</sup> The particle size distribution of a normal sample synthesized at 55 °C is shown in the Supporting Information (Figure S9). The silica flocs/particles are formed in a solution containing amphiphilic molecules (Pluronic block copolymers), and it is likely that Pluronic polymers decorate the surface of the flocs/particles.

(ii) Changing the properties of the solution, either by addition of salt<sup>20</sup> or by dilution,<sup>15</sup> at the time when the oriented aggregation occurs, affects the aggregation behavior. The fact that the properties of the solution, such as salt content, have an effect on the aggregation indicates that the source of stability is dependent on this parameter. Pluronic polymers, and polyethylenoxide in general, are known to be strongly dependent on salt content and also dependent on the identity of the ions.<sup>36</sup>

Based on this, we propose a hypothesis rationalizing the colloidal stability as largely dependent on Pluronic polymers (i.e., the polyethyleneoxide blocks) decorating the flocs/particles. In a previous <sup>1</sup>H NMR of the formation of SBA-15 using P123 as structure director, it was concluded that, after completed synthesis, a soluble fraction of a short and/or EO-rich polymer fraction remains in solution, i.e. a fraction that is not incorporated in the flocs/particles.<sup>37</sup> Further, it is known that there is a positive interaction between EO-polymers and silica;<sup>19,38,39</sup> in fact, it is this interaction that drives the current synthesis. EO-rich polymers are expected to associate with siliceous surfaces, such as those of the flocs/particles. In an ellipsometry study,<sup>19</sup> Pluronic polymers were found to adhere to silica surfaces in a way similar to that of EO-polymers regardless of the length of the PPO-block. It was also shown that the PO segments are preferentially located in the middle region of the adsorbed layer. It is thus expected that the Pluronic polymer (or fractions of these) protrudes from the surface of the flocs into the solution. These Pluronic polymers are probably accompanied by silica oligomers/polymers that have been suggested to be the stabilizing component for silica sols<sup>30</sup> (see Introduction). The polymeric (Pluronic and silica) brush-layer will impose steric stabilization of the flocs/particles that would be dependent on parameters affecting the solubility of the polyethyleneoxide.

Figure 5 (and Supporting Information Scheme S3) shows a schematic representation of the flocs represented by gray spheres, decorated with a polymer brush layer. For simplicity, the brushes viewed from the side are depicted as twisting lines and brushes depicted in other directions are shown as dots.

If, to a first approximation, the flocs grow until the solution is more or less drained of silica species and Pluronics (i.e., silica decorated micelles), growth would cease if the flocs became colloidally stable in the process. However the cryo-TEM results clearly show that flocs coalesce in a seemingly arbitrary manner



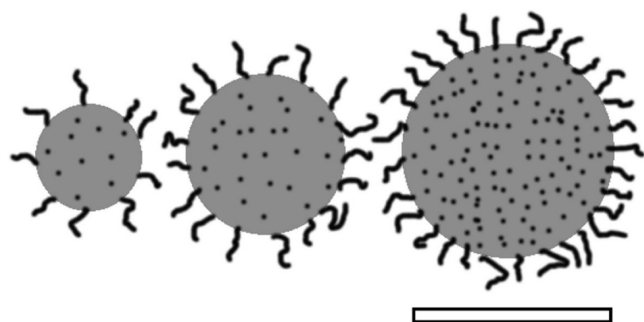


**Figure 5.** Schematic of the growth of globular flocs. As the flocs grow larger via agglomeration, the number density of polymer brushes increases, eventually leading to a repulsive force being dominant, resulting in (transient) colloidal stability. The polymer brushes are depicted as twisting lines from the side. The dotted pattern depicts brushes viewed more or less from the top. The brushes are not drawn to scale. Scale bar  $\approx 1 \mu\text{m}$ .

(see Figure 3), which, typically, would produce a material with a large variation in particle sizes. If, however, the colloidal stability increases with floc size, the size will be regulated and growth will cease when a limiting stability is reached. Flocs will grow until the coverage of the polymer brush layer is sufficient to provide steric stability (as depicted in the schematic shown in Figure 5). Floc growth, and coalescence of flocs, leads to a decrease of the area (total area of the interface between flocs and surrounding solution) to volume (total volume of the flocs) ratio, and as the flocs at this stage (around 6–14 min) are still liquid-like, the brushes are expected to be able to relocate and maintain a position at the interface (i.e., decorating the surface of the floc). The coverage of brushes on the external surface will in this process increase (see Figure 5). This will result in a more potent repulsive force and a gradual increase in the colloidal stability. Eventually the flocs reach a limiting size where the colloidal stability prevents further coalescence.

With time, however, it is observed that particles, as mentioned above, always aggregate in an unspecific manner, indicating that the colloidal stability is of a transient nature. This may be due to the brushes getting more restricted as the silica connectivity increases, or it may be a result of more silica oligomers from solution being deposited on the PEO-chains in the brush, or it may possibly result from both of these effects. Both scenarios would cause a decrease in the steric repulsion and thus facilitate further aggregation.

The specific aggregation was previously explained as a consequence of the energetics of the specific surfaces.<sup>15</sup> The difference in energetics could stem from an analogous effect to the above. As the flocs start to become ordered, some of the crystallographically equivalent surfaces may become void of, or at least have lower, coverage of the stabilizing brushes, leading to certain surfaces being “sticky”, prompting the oriented aggregation.

If the colloidal stability is the main control to growth of flocs, alterations affecting the colloidal stability should affect their growth. The Pluronic block copolymers seem to be the preferred molecules to target, as the solubility of the polyethyleneoxid can be regulated. The silica part of the brushes on the other hand is involved in an ongoing reaction, successively changing toward a more rigid network.

A number of experiments were performed in order to test the hypothesis at the stages when the flocs are in the process of growing but prior to the oriented aggregation step. We used

three approaches, all targeting the Pluronic molecules (i.e., the PEO part of the block copolymer).

(1) Addition of salt (with salting-out properties). NaCl was added to the ongoing synthesis. Chloride ions are known to dehydrate the PEO chains,<sup>40</sup> and the Pluronic brushes decorating the silica flocs would thus shrink, leading to a decrease in the colloidal stability.

(2) Addition of extra Pluronic. More Pluronic, both P104 and F108, was added around the time for the oriented aggregation. More Pluronic decorating the flocs is expected to increase the colloidal stability.

(3) Addition of silica oligomers. There is a hydrophobic attraction between the PEO segments of the Pluronic molecules and the silica oligomers,<sup>11</sup> and the affinity of the silica species to the PEO segments is expected to increase with the degree of silica polymerization. A sudden increase in concentration of silica oligomers is expected to destabilize the flocs and affect the aggregation behavior of the system.

**1. Addition of NaCl.** NaCl was added at 7, 8, 9, 10, 11, and 12 min, respectively, after TMOS addition initiated the synthesis, giving a final concentration in the solution of 0.01, 0.1, 0.25, and 0.5 M respectively. Figure 6 shows the particles

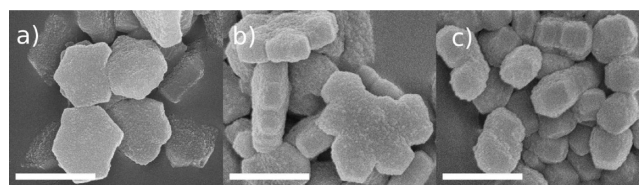


**Figure 6.** SEM images showing (a) normal particles, (b) particles where the primary particle structure is clearly visible due to addition of NaCl at  $t = 11$  min, and (c) smaller primary particles instantly precipitated due to NaCl addition at  $t = 12$  min. The synthesis temperature was  $55^\circ\text{C}$  in all cases. Scale bar =  $1 \mu\text{m}$ .

obtained when (a) no salt was added, i.e. a normal synthesis, (b) NaCl (obtaining a 0.25 M solution) was added at 11 min, and (c) NaCl (obtaining a 0.25 M solution) was added at 12 min. (More micrographs are shown in Supporting Information Figure S10.)

Additions made at 7–11 min produce particles with morphology consistent with having experienced an oriented aggregation step (Figure 6b), whereas addition made at 12 min produces primary particles (Figure 6c) which has been explained to result from an instant precipitation, impeding the oriented aggregation.<sup>20</sup> When the oriented aggregation occurs, some faces are energetically unstable and the association of these lead to the formation of secondary particles (cf. Introduction). Addition of a substantial amount of NaCl destabilizes all faces and leads to unspecific aggregation and precipitation. If, however, the same salt addition is made earlier, during the growth and coalescing of flocs, the oriented aggregation step does occur. A closer comparison of the particles obtained after this addition and the ones obtained from a normal synthesis reveals clear differences. Additions of salt produces secondary particles but with a less uniform particle morphology (Figure 6b). The particles are not always heptamers, and the variation of sizes of the “building stones” is greater. This is also consistent with the assumption that NaCl reduces the colloidal stability, as manifested in the observed earlier time of precipitation (see SI Figure S11). The oriented aggregation is forced to occur prior to the uniform floc size

being reached; hence, there is a larger size variation of the “building stones” (cf. the cryo-TEM micrographs in Figure 3c).

**2. Addition of Pluronic.** We also added Pluronic molecules, P104 and F108, respectively, aiming at increasing the colloidal stability. In SI Figure S12, particles synthesized at 50 °C with the addition of extra P104 polymer (5.0 and 10 wt % with respect to the original amount of Pluronics) at a time equivalent to those of the salt addition at 55 °C,<sup>7</sup> are shown. In SI Figure S13, particles synthesized at 55 °C with addition of F108 (1.0 and 2.5 wt % with respect to the original amount of Pluronics P104) 10 min after initiation are shown.

Addition of extra polymer (P104 or F108) affects both the aspect ratio and the size of the produced particles (see SI Figures S12, S13, and S14). This is consistent with the idea that the polymers “arrange” at the surface of the flocs and play an important role in determining the surface energies for the different emerging crystallographic faces. The crystallographic difference between the 001 faces and the faces perpendicular to these are expected to induce a variation in the arrangement of the Pluronic molecules at the corresponding silica water interface which is manifested in the change of aspect ratio in the particles. It was previously demonstrated that such changes may result by varying synthesis conditions.<sup>21</sup> In SI Figure S14 the particle size variations for different Pluronic additions are shown. Clearly the particles size is dependent on these additions, and the more Pluronics present, the smaller are the particles obtained. This is consistent with the scheme presented in Figure 5; the colloidal stability increases as more Pluronic molecules gather at the interface. A further effect of the polymer addition is the observed delay of the precipitation, also consistent with a higher colloidal stability. Once a critical limit of the added amount of Pluronic polymer is reached, the influence is so large that both ordered structure and morphology are lost.

**3. Addition of Silica.** Another strategy for testing the hypothesis is to add a small amount of silica oligomers. To a normal synthesis at 50 °C, a small amount (1 mL) of a 1.6 M HCl solution containing silica oligomers was added. The silica oligomers are produced by adding TMOS to 1.6 M HCl and allowing for hydrolysis and condensation for specific times (15–75 min). The size of the oligomers is expected to be determined by the length of hydrolysis and condensation. The strength of interaction is expected to be dependent on the size of the silica oligomers, with larger oligomers having stronger interaction.

The additions typically lead to a faster precipitation, and an instant precipitation was observed when the TMOS had prehydrolyzed for 75 min. The additions also led to an increased oriented aggregation, shown in SI Figure S15 by the large platelike particles. This confirms that the addition of silica caused an increase in aggregation, likely caused by a decrease in the colloidal stability of the flocs. This decrease can be the consequence of either the fact that the Pluronic brushes are less efficient stabilizers when silica oligomers have attached to the brushes or, possibly, that the silica oligomers create a bridging effect between flocs. The magnitude of the response depends on both the reaction time of the silica solution (i.e., the size of the oligomers) and the added amount, but typically the qualitative effect is the same. The particle size distribution of the particles obtained with silica oligomer additions is shown in SI Figure S16.

These three series of experiments (addition of NaCl, P104/F108, and silica oligomers) all support the hypothesis that

Pluronic block-copolymers decorate the surface of the flocs and that the colloidal stability is dependent on the strength of the steric stabilization caused by the Pluronic polymer. It should also be noted that in all cases the expected high-quality SBA-15 structure was obtained (SI Figure S17 shows TEM micrographs of some of the materials). The strength of stabilization is dependent on the coverage of polymers as well as on the thickness of the brush-layer. Please note that it is likely that the brush layer is composed of both Pluronics and silica, but in these experiments only the Pluronics molecules were targeted.

## CONCLUSIONS

We have shown by direct imaging (cryo-TEM) of the solution wherein SBA-15 forms that the initial stages of formation of this mesoporous material occur via floc formation, as has been previously reported.<sup>11</sup> We have seen no indication of the presence of elongated micelles in the solution. A hypothesis for the nature of growth control and (transient) colloidal stability of the flocs/particles was presented and tested. The stability and growth is suggested to be controlled mainly by the presence of PEO-polymers decorating the floc surface.

## ASSOCIATED CONTENT

### Supporting Information

Additional schematics, UV-vis and DLS-data, as well as more cryo-TEM and SEM images. This material is available free of charge via the Internet at <http://pubs.acs.org>.

## AUTHOR INFORMATION

### Present Address

<sup>†</sup>Graduate School of Frontier Biosciences, Osaka University, 1-3 Yamadaoka, Suita, Osaka 565-0871, Japan.

### Notes

The authors declare no competing financial interest.

## ACKNOWLEDGMENTS

We acknowledge financial support by the Swedish Research Council (VR) through the Linnaeus grant Organizing Molecular Matter (OMM) center of excellence (239-2009-6794), through project grant (80475801), and the Swedish Foundation for Strategic Research (RMA08-0056). We are also indebted to Gunnel Karlsson for skilled support with the cryo-TEM studies and professor Håkan Wennerström for valuable discussions.

## REFERENCES

- (1) Rosenholm, J. M.; Sahlgren, C.; Linden, M. Towards multifunctional, targeted drug delivery systems using mesoporous silica nanoparticles - opportunities & challenges. *Nanoscale* **2010**, *2*, 1870–1883.
- (2) Choi, M.; Kleitz, F.; Liu, D.; Lee, H. Y.; Ahn, W.; Ryoo, R. Controlled polymerization in mesoporous silica toward the design of organic-inorganic composite nanoporous materials. *J. Am. Chem. Soc.* **2005**, *127*, 1924–1932.
- (3) Kalbasi, R. J.; Kolahdoozan, M.; Rezaei, M. Synthesis and characterization of PVAm/SBA-15 as a novel organic-inorganic hybrid basic catalyst. *Mater. Chem. Phys.* **2011**, *125*, 784–790.
- (4) Manet, S.; Schmitt, J.; Imperor-Clerc, M.; Zholobenko, V.; Durand, D.; Oliveira, C. L. P.; Pedersen, J. S.; Gervais, C.; Baccile, N.; Babonneau, F.; Grillo, I.; Meneau, F.; Rochas, C. Kinetics of the Formation of 2D-Hexagonal Silica Nanostructured Materials by Nonionic Block Copolymer Templating in Solution. *J. Phys. Chem. B* **2011**, *115*, 11330–11344.

- (5) Ruthstein, S.; Frydman, V.; Kababya, S.; Landau, M.; Goldfarb, D. Study of the Formation of Mesoporous Material SBA-15 by EPR Spectroscopy. *J. Phys. Chem. B* **2003**, *107*, 1739–1748.
- (6) Ruthstein, S.; Schmidt, J.; Kesselman, E.; Talmon, Y.; Goldfarb, D. Resolving intermediate solution structures during the formation of mesoporous SBA-15. *J. Am. Chem. Soc.* **2006**, *128*, 3366–3374.
- (7) Linton, P.; Rennie, A. R.; Zackrisson, M.; Alfredsson, V. In-situ observation of the genesis of mesoporous silica on scales from 1 nm to 1  $\mu$ m. *Langmuir* **2009**, *25*, 4685–4691.
- (8) Sundblom, A.; Palmqvist, A. E. C.; Holmberg, K. Study of the Pluronic-Silica Interaction in Synthesis of Mesoporous Silica under Mild Acidic Conditions. *Langmuir* **2009**, *26*, 1983–1990.
- (9) Sundblom, A.; Oliveira, C. L. P.; Pedersen, J. S.; Palmqvist, A. E. C. On the formation mechanism of Pluronic-templated mesostructured silica. *J. Phys. Chem. C* **2010**, *114*, 3483–3492.
- (10) Flodström, K.; Teixeira, C. V.; Amenitsch, H.; Alfredsson, V.; Lindén, M. In Situ Synchrotron Small-Angle X-ray Scattering/X-ray Diffraction Study of the Formation of SBA-15 Mesoporous Silica. *Langmuir* **2004**, *20*, 4885–4891.
- (11) Flodström, K.; Wennerström, H.; Alfredsson, V. Mechanism of Mesoporous Silica Formation. A Time-Resolved NMR and TEM Study of Silica-Block Copolymer Aggregation. *Langmuir* **2004**, *20*, 680–688.
- (12) Linton, P.; Rennie, A. R.; Alfredsson, V. Evolution of structure and composition during the synthesis of mesoporous silica SBA-15 studied by small-angle neutron scattering. *Solid State Sci.* **2011**, *13*, 793–799.
- (13) Khodakov, A. Y.; Zholobenko, V. L.; Imperor-Clerc, M.; Durand, D. Characterisation of the initial stages of SBA-15 synthesis by in situ time-resolved small-angle x-ray scattering. *J. Phys. Chem. B* **2005**, *109*, 22780–22790.
- (14) Che, R.; Gu, D.; Shi, L.; Zhao, D. Direct imaging of the layer-by-layer growth and rod-unit repairing defects of mesoporous silica SBA-15 by cryo-SEM. *J. Mater. Chem.* **2011**, *21*, 17371–17381.
- (15) Linton, P.; Alfredsson, V. Growth and Morphology of Mesoporous SBA-15 Particles. *Chem. Mater.* **2008**, *20*, 2878–2880.
- (16) Zholobenko, V. L.; Khodakov, A. Y.; Imperor-Clerc, M.; Durand, D.; Grillo, I. Initial stages of SBA-15 synthesis: An overview. *Adv. Colloid Interface Sci.* **2008**, *142*, 67–74.
- (17) Yu, C.; Fan, J.; Tian, B.; Zhao, D. Morphology Development of Mesoporous Materials: a Colloidal Phase Separation Mechanism. *Chem. Mater.* **2004**, *16*, 889–898.
- (18) Mesa, M.; Sierra, L.; Guth, J.-L. Contribution to the study of the formation mechanism of mesoporous SBA-15 and SBA-16 type silica particles in aqueous acid solutions. *Microporous Mesoporous Mater.* **2008**, *112*, 338–350.
- (19) Malmsten, M.; Linse, P.; Cosgrove, T. Adsorption of PEO-PPO-PEO block copolymer at silica. *Macromolecules* **1992**, *25*, 2474–2481.
- (20) Linton, P.; Wennerström, H.; Alfredsson, V. Controlling particle morphology and size in the synthesis of mesoporous SBA-15 materials. *Phys. Chem. Chem. Phys.* **2010**, *12*, 3852–3858.
- (21) Linton, P.; Hernandez-Garrido, J. C.; Midgley, P. A.; Wennerström, H.; Alfredsson, V. Morphology of SBA-15 - directed by association processes and surface energies. *Phys. Chem. Chem. Phys.* **2009**, *11*, 10973–10982.
- (22) Cölfen, H.; Antonietti, M. *Mesocrystals and Nonclassical Crystallization: New Self-assembled Structures*; John Wiley & Sons Ltd.: Chichester, 2008; pp 113–233.
- (23) Chen, X.; Qiao, M.; Xie, S.; Fan, K.; Zhou, W.; He, H. Self-construction of core-shell and hollow zeolite analcime icositetrahedra: a reversed crystal growth process via oriented aggregation of nanocrystallites and recrystallization from surface to bulk. *J. Am. Chem. Soc.* **2007**, *129*, 13305–13312.
- (24) Zhang, H.; Sun, J.; Ma, D.; Weinberg, G.; Su, D. S.; Bao, X. Engineered complex emulsion system: toward modulating pore length and morphological architecture of mesoporous silicas. *J. Phys. Chem. B* **2006**, *110*, 25908–25915.
- (25) Shen, S.; Chen, F.; Chow, P. S.; Phanapavudhikul, P.; Zhu, K.; Tan, R. B. H. Synthesis of SBA-15 mesoporous silica via dry-gel conversion route. *Microporous Mesoporous Mater.* **2006**, *92*, 300–308.
- (26) Fahn, Y.-Y.; Su, A.-C.; Shen, P. Towerlike SBA-15: Base and (10)-Specific Coalescence of a Silicate-Encased Hexagonal Mesophase Tailored by Nonionic Triblock Copolymers. *Langmuir* **2005**, *21*, 431–436.
- (27) Hsu, Y.-C.; Hsu, Y.-T.; Hsu, H.-Y.; Yang, C.-M. Facile Synthesis of Mesoporous Silica SBA-15 with Additional Intra-particle Porosities. *Chem. Mater.* **2009**, *19*, 1120–1126.
- (28) Kosuge, K.; Sato, T.; Kikukawa, N.; Takemori, M. Morphological control of rod- and fiberlike SBA-15 type mesoporous silica using water-soluble sodium silicate. *Chem. Mater.* **2004**, *16*, 899–905.
- (29) Kubo, S.; Kosuge, K. Salt-induced Formation of Uniform Fiberlike SBA-15 Mesoporous Silica Particles and Application to Toluene Adsorption. *Langmuir* **2009**, *23*, 11761–11768.
- (30) Bergna, H., E., Roberts, W. O., Eds. *Colloidal Silica. Fundamentals and Application*; Taylor & Francis Group: Boca Raton, FL, 2006; Vol. 131, pp 19–21.
- (31) Zhao, D.; Huo, Q.; Feng, J.; Chmelka, B. F.; Stucky, G. D. Nonionic Triblock and Star Diblock Copolymer and Oligomeric Surfactant Syntheses of Highly Ordered, Hydrothermally Stable, Mesoporous Silica Structures. *J. Am. Chem. Soc.* **1998**, *120*, 6024–6036.
- (32) Bellare, J. R.; Davis, H. T.; Scriven, L. E.; Talmon, Y. Controlled Environment Vittrification System - An Improved Sample Preparation Technique. *J. Electron Microsc. Tech.* **1988**, *10*, 87–111.
- (33) Lee, H. I.; Kim, J. H.; Stucky, G. D.; Shi, Y.; Pak, C.; Kim, J. M. Morphology-selective synthesis of mesoporous SBA-15 particles over micrometer, submicrometer and nanometer scales. *J. Mater. Chem.* **2010**, *20*, 8483–8487.
- (34) Boissière, C.; Larbot, A.; Bourgaux, C.; Prouzet, E.; Bunton, C. A. A Study of the Assembly Mechanism of the Mesoporous MSU-X Silica Two-Step Synthesis. *Chem. Mater.* **2001**, *13*, 3580–3586.
- (35) Sundblom, A.; Oliveira, C. L. P.; Palmqvist, A. E. C.; Pedersen, J. S. Modeling in Situ Small-Angle X-ray Scattering Measurements Following the Formation of Mesostructured Silica. *J. Phys. Chem. C* **2009**, *113*, 7706–7713.
- (36) Alexandridis, P.; Holzwarth, J. F. Differential Scanning Calorimetry Investigation of the Effect of Salts on Aqueous Solution Properties of an Amphiphilic Block Copolymer (Pluronic). *Langmuir* **1997**, *13*, 6074–6082.
- (37) Flodström, K.; Teixeira, C. V.; Amenitsch, H.; Alfredsson, V.; Lindén, M. In Situ Synchrotron Small-Angle X-ray Scattering/X-ray Diffraction Study of the Formation of SBA-15 Mesoporous Silica. *Langmuir* **2004**, *20*, 4885.
- (38) Dijt, J. C.; Cohen Stuart, M. A.; Hofman, J. E.; Fleer, G. J. Kinetics of polymer adsorption in stagnation point flow. *J. Colloids Surf.* **1990**, *51*, 141.
- (39) Howard, G. J.; McConnell, P. Adsorption of polymers at the solution-solid interface I. Polyethers on silica. *J. Phys. Chem.* **1967**, *71*, 2974.
- (40) Kabalnov, A.; Olsson, U.; Wennerström, H. Salt Effects on Nonionic Microemulsions Are Driven by Adsorption/Depletion at the Surfactant Monolayer. *J. Phys. Chem.* **1995**, *99*, 6220–6230.